Effect of discrete breathers on macroscopic properties of the Fermi-Pasta-Ulam chain

Preprint · July 2019

CITATIONS
0

READS
97

8 authors, including:

E. A. Korznikova
Institute for Metals Superplasticity Problems of Russian Academy of Sciences
116 PUBLICATIONS **1,289** CITATIONS
SEE PROFILE

Anton M. Krivtsov
Peter the Great St.Petersburg Polytechnic University
140 PUBLICATIONS **1,249** CITATIONS
SEE PROFILE

Vitaly Kuzkin
Peter the Great St.Petersburg Polytechnic University
48 PUBLICATIONS **280** CITATIONS
SEE PROFILE

Vakhid Gani
National Research Nuclear University MEPhI
58 PUBLICATIONS **723** CITATIONS
SEE PROFILE

Effect of discrete breathers on macroscopic properties of the Fermi-Pasta-Ulam chain

Elena A. Korznikova[1],* Alina Y. Morkina[2],† Mohit Singh[3],‡ Anton M. Krivtsov[4,5],§
Vitaly A. Kuzkin[4,5],¶ Vakhid A. Gani[6,7],** Yuri V. Bebikhov[8],†† and Sergey V. Dmitriev[1,9‡‡]
[1]*Institute of Molecule and Crystal Physics, Ufa Federal Research Centre of the Russian Academy of Sciences, Ufa 450054, Russia*
[2]*Ufa State Aviation Technical University, Ufa 450008, Russia*
[3]*Indian Institute of Technology Kharagpur, Kharagpur 721302, India*
[4]*Peter the Great Saint Petersburg Polytechnical University, Polytechnicheskaya Street 29, Saint Petersburg, Russia*
[5]*Institute for Problems in Mechanical Engineering RAS, Bolshoy pr. V.O. 61, Saint Petersburg, Russia*
[6]*Department of Mathematics, National Research Nuclear University MEPhI (Moscow Engineering Physics Institute), Moscow 115409, Russia*
[7]*Theory Department, National Research Center Kurchatov Institute, Institute for Theoretical and Experimental Physics, Moscow 117218, Russia*
[8]*North-Eastern Federal University, Polytechnic Institute (branch) in Mirny, 678170 Mirny, Sakha (Yakutia), Russia*
[9]*National Research Tomsk State University, Tomsk 634050, Russia*

For a number of crystals the existence of spatially localized nonlinear vibrational modes, called discrete breathers (DBs) or intrinsic localized modes (ILMs), has been demonstrated using molecular dynamics and in a few cases the first-principle simulations. High-resolution imaging of DBs is a challenging task due to their relatively short lifetime ranging typically from 10 to 10^3 atomic oscillation periods (1 to 100 ps). An alternative way to prove the existence of DBs is to evaluate their impact on the measurable macroscopic properties of crystals. In the present study, we analyze the effect of DBs on macroscopic properties of the Fermi-Pasta-Ulam chain with symmetric and asymmetric potentials. The specific heat, thermal expansion (stress), and Young's modulus are monitored during the development of modulational instability of the zone boundary mode. The instability results in the formation of chaotic DBs followed by the transition to thermal equilibrium when DBs disappear due to energy radiation in the form of small-amplitude phonons. Time evolution of the macroscopic properties during this transition is monitored. It is found that DBs reduce the specific heat for all the considered chain parameters. They increase the thermal expansion when the potential is asymmetric and, as expected, thermal expansion is not observed in the case of symmetric potential. The Young's modulus in the presence of DBs is smaller than in thermal equilibrium for the symmetric potential and for the potential with a small asymmetry, but it is larger than in thermal equilibrium for the potential with greater asymmetry.

PACS numbers: 05.45.Yv, 63.20.-e
Keywords: Crystal lattice, Fermi-Pasta-Ulam chain, modulational instability, discrete breather, intrinsic localized mode, specific heat, thermal expansion, Young's modulus

I. INTRODUCTION

Discrete breathers (DBs), also called intrinsic localized modes (ILMs), are spatially localized, large-amplitude oscillatory modes in nonlinear lattices free of defects. Discovery of DBs in nonlinear lattices three decades ago [1–3] has triggered extensive studies devoted to the phenomenon of vibrational energy localization [4, 5]. Experimentally DBs have been excited in the physical systems of different nature, e.g., in macroscopic arrays of coupled pendula or magnets [6–8], granular crystals [9–16], cantilever arrays [17–19], electrical lattices [20–22], optical waveguide arrays [23], Josephson junction arrays [24, 25], etc. DBs can be found in crystal lattices [26], as confirmed by measuring vibrational spectra for alpha-uranium [27–29], helium [30], NaI [31, 32], graphite [33], and PbSe [34]. On the other hand, these experimental results in some cases can be interpreted in different ways and they are still debated [35].

At present, computer simulation methods play a very important role in the study of DB properties in various crystals. With the help of *ab initio* simulations, the existence of DBs in strained graphene and graphane has been confirmed [36, 37]. With the help of molecular dynamics method DBs have been studied in the ionic crystals [38–40], monoatomic Morse lattices [41, 42], covalent crystals [43, 44], metals [45–51], ordered alloys [52–55], carbon and hydrocarbon nanomaterials [56–68], boron nitride [69], and proteins [70–73].

It is of great importance to understand how DBs affect macroscopic properties of crystals [74]. In the experimental studies, anomalies in thermal expansion [29]

*Electronic address: elena.a.korznikova@gmail.com
†Electronic address: alinamorkina@yandex.ru
‡Electronic address: mohitsingh1997@gmail.com
§Electronic address: akrivtsov@bk.ru
¶Electronic address: kuzkinva@gmail.com
**Electronic address: vagani@mephi.ru
††Electronic address: bebikhov.yura@mail.ru
‡‡Electronic address: dmitriev.sergey.v@gmail.com

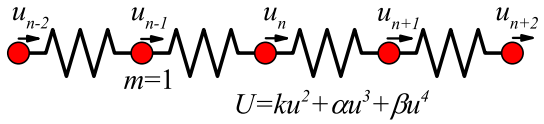

Figure 1: FPU chain of harmonically coupled, unit mass point-wise particles interacting with the quartic polynomial on-site potential with the nearest neighbours.

and heat capacity [27] of alpha-uranium at high temperatures were attributed to excitation of DBs. In the numerical study [76] it was shown that DBs are responsible for the transition from ballistic to normal heat conduction in a nonlinear chain. DBs increase (decrease) specific heat of the nonlinear chain with soft (hard) type nonlinearity on-site potential and harmonic nearest-neighbour coupling [77].

For a chain with on-site potential, one cannot calculate the effect of DBs on thermal expansion and on elastic constants. That is why, in the present study, the Fermi-Pasta-Ulam (FPU) chain is considered and these macroscopic properties are calculated together with the specific heat. For this we use the same approach as in [77], namely, we simulate the modulational instability of the zone boundary mode ($q = \pi$) which leads first to energy localization in the form of long-lived DBs and subsequent transition to thermal equilibrium [20, 83–87]. The macroscopic characteristics of the chain in the regime when energy is localized on DBs are compared with that in thermal equilibrium, thus revealing the effect of DBs on those properties.

We note that properties of DBs in the FPU chain have been analyzed by Flach and Gorbach in [88].

In Sec. II the model and simulation details are described. The simulation results on modulational instability of the zone-boundary mode and macroscopic properties of the chain are presented in Sec. III. Our conclusions are presented in Sec. IV.

II. THE MODEL AND SIMULATION SETUP

We consider the FPU chain of particles having mass m (see Fig. 1) described by the Hamiltonian

$$H = K + P = \sum_n \frac{m\dot{u}_n^2}{2} + \sum_n U(u_{n+1} - u_n), \qquad (1)$$

where K is the kinetic energy, P is the potential energy, u_n is the displacement of the n-th particle from its equilibrium position and $\dot{u}_n$ is its velocity (overdot means derivative with respect to time t). The particles are coupled to their nearest neighbors by the anharmonic bonds

$$U(\xi) = \frac{k}{2}\xi^2 + \frac{\alpha}{3}\xi^3 + \frac{\beta}{4}\xi^4, \qquad (2)$$

where k is the coefficient in front of the harmonic term, while the coefficients α and β define the contributions from the cubic and quartic terms, respectively.

Without loss of generality, we set m=1 and $k = 1$. We take $\beta = 3$ and consider three different values for α, namely, $\alpha = \{0, -1/4, -1/2\}$. For $\alpha = 0$ the potential is symmetric, while for the chosen negative values of α it is an asymmetric single-well potential.

From the Hamiltonian defined above, the following equation of motion can be derived

$$\begin{aligned} m\ddot{u}_n &= k(u_{n-1} - 2u_n + u_{n+1}) \\ &+ \alpha[(u_{n+1} - u_n)^2 - (u_n - u_{n-1})^2] \\ &+ \beta[(u_{n+1} - u_n)^3 - (u_n - u_{n-1})^3]. \end{aligned} \qquad (3)$$

The Störmer method of order six with the time step $\tau = 10^{-3}$ is used for numerical integration of these equations. With such a time step, the relative change in total energy of the chain in a typical numerical run is not greater than 10^{-5}.

Substituting the ansatz $u_n \sim \exp[i(qn - \omega_q t)]$ into Eq. (3) with $\alpha = \beta = 0$, one finds the relation between wave number q and frequency ω_q for the small-amplitude normal modes in the form

$$\omega_q^2 = \frac{2k}{m}(1 - \cos q). \qquad (4)$$

The phonon band of the chain ranges from $\omega_{\min} = 0$ for $q = 0$ to $\omega_{\max} = 2$ for $q = \pm\pi$.

Here, a chain of $N = 2048$ particles is considered. Test runs with larger number of particles produced nearly same results.

Initial conditions are set in the form of the zone-boundary mode ($q = \pi$) with the amplitude A,

$$u_n = A\sin(\pi n - \omega_{\max} t). \qquad (5)$$

If A is not too small, the above mode is modulationally unstable. At $t = 0$, all the particles have the same energy but the instability results in energy localization which can be characterized by the localization parameter

$$L = \frac{\sum e_n^2}{\left(\sum e_n\right)^2}, \qquad (6)$$

where

$$e_n = \frac{m\dot{u}_n^2}{2} + \frac{1}{2}U(u_{n+1} - u_n) + \frac{1}{2}U(u_n - u_{n-1}), \qquad (7)$$

is the energy of the n-th particle.

We define temperature as the averaged kinetic energy per atom,

$$T = \bar{K} = \frac{1}{N}\sum_n \frac{m\dot{u}_n^2}{2}. \qquad (8)$$

Heat capacity of the chain is defined as

$$C = \lim_{\Delta T \to \infty} \frac{\Delta H}{\Delta T}, \qquad (9)$$

where ΔH is the increment in energy of the chain and ΔT is the corresponding increment in temperature. The specific heat capacity (or simply specific heat) is the heat capacity per particle. Periodic boundary conditions are used meaning that the specific heat at constant volume is calculated.

In our simulations, total energy H is conserved, so that Eq. (9) cannot be used. We characterize the specific heat of the chain at constant volume by the ratio

$$c_V = \frac{\bar{H}}{\bar{K}}, \tag{10}$$

where $\bar{H}$ and $\bar{K}$ are the total energy and the kinetic energy of the chain per atom, respectively.

In linear systems $\bar{H} = 2\bar{K}$ and $c_V = 2$. Due to nonlinearity, the kinetic energy can differ from the potential energy resulting in deviation of c_V from this value.

In the following section, the time evolution of localization parameter, specific heat, stress in the chain and Young's modulus of the chain have been calculated. These macroscopic characteristics have been compared in the regime of energy localization by DBs with those in thermal equilibrium.

III. MODULATIONAL INSTABILITY

We excite the zone-boundary mode Eq. (5) in the chain considering various amplitudes A. While integrating the equations of motion Eq. (3), we monitor the change in the localization parameter L, Eq. (6), specific heat c_V, Eq. (10), stress and Young's modulus.

A. Energy localization

Localization parameter as the function of time is presented in Fig. 2 for various values of A and three values of the potential asymmetry parameter α. At $t = 0$, all curves start from the minimal possible value of the localization parameter that is $L = 1/N = 0.49 \times 10^{-3}$. The development of modulational instability results in energy localization due to the formation of DBs and this leads to an increase in the localization parameter. DBs slowly radiate their energy and thus, the localization parameter gradually decreases and in the end, when the system reaches the state of thermal equilibrium, L oscillates near the small value of 1.8×10^{-3}.

Distribution of energy over the chain at the time when localization parameter is maximal is shown in Fig. 3 for various values of the potential asymmetry parameter α from $\alpha = 0$ in (a) to $\alpha = -0.5$ in (c). One can see the sets of sharply localized DBs.

The time evolution of the number of DBs produced, $N_{\rm DB}$, and the corresponding average DB energy, $E_{\rm DB}$, are shown in Fig. 4 and Fig. 5, respectively, for different values of the zone-boundary mode amplitudes A and for

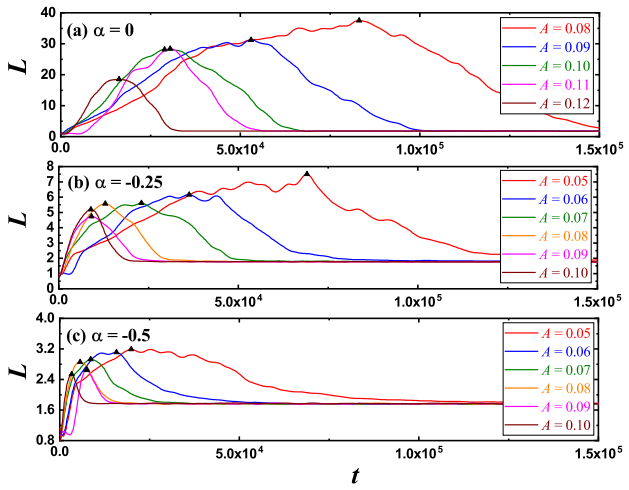

Figure 2: Localization parameter as the function of time for various amplitudes of the initially excited zone-boundary mode, A. For all cases at $t = 0$ the localization parameter is $L = 1/N = 0.49 \times 10^{-3}$. Modulational instability results in increase of L due to energy localization on DBs. Then L decreases because DBs gradually radiate energy and eventually system reaches thermal equilibrium with L oscillating near the value of 1.8×10^{-3}. The points of maxima of L are marked with triangles.

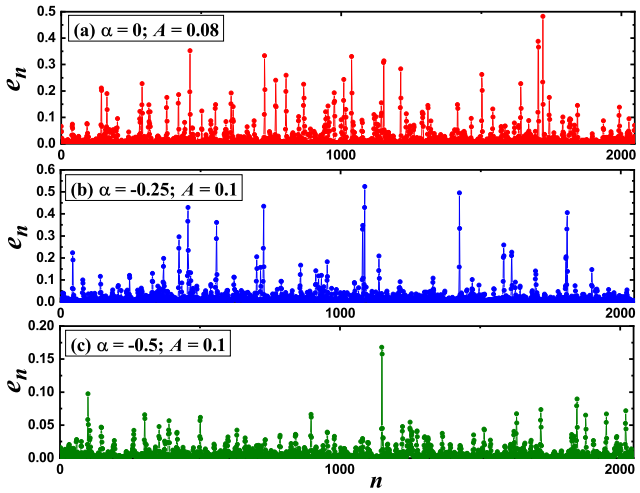

Figure 3: Total energies of particles in the chain at the time when the localization parameter reaches its maximum for different values of the potential asymmetry parameter α, as indicated in each panel.

three value of the potential asymmetry parameter α. In these plots, by triangles we indicate the points when the localization parameter L reaches its maximum. It can be seen from Fig. 4 that the maximal number of DBs for $\alpha = 0$ very weakly depends on A and for the negative values of α maximal values of $N_{\rm DB}$ are somewhat greater for larger A. The same can be said about the maximal DB energy: it weakly depends on A for $\alpha = 0$ and increases with A for negative α.

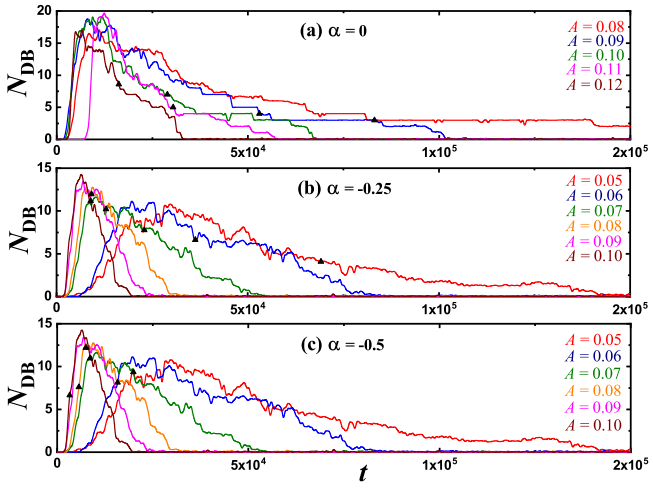

Figure 4: Number of DBs as the function of time for various amplitudes of the initially excited zone-boundary mode at different values of the potential asymmetry parameter α. Triangles indicate the points of maximal localization parameter.

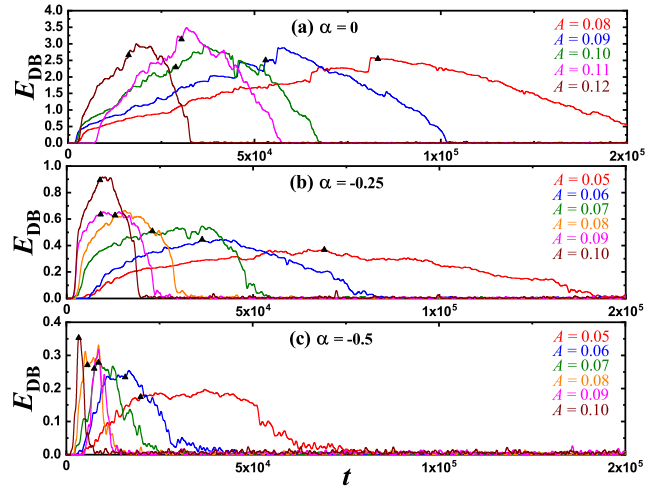

Figure 5: Average DB energy as the function of time for various amplitudes of the initially excited zone-boundary mode at different values of the potential asymmetry parameter α. Triangles indicate the points of maximal localization parameter.

From Fig. 4 one can also see that N_{DB} reaches its maximum well before the localization parameter L becomes maximal for the case of $\alpha = 0$ and $\alpha = -0.25$, but when $\alpha = -0.5$, first L reaches a maximal value and then N_{DB}. As for E_{DB}, as shown in Fig. 5, the time when it attains maximal value is close to the time when L is maximal.

It is also worth pointing out that the maximal number of DBs, i.e. N_{DB}, weakly depends on the values of α (see Fig. 4), whereas the maximal DB energy, E_{DB}, rapidly decreases with increasing asymmetry of the potential (see Fig. 5).

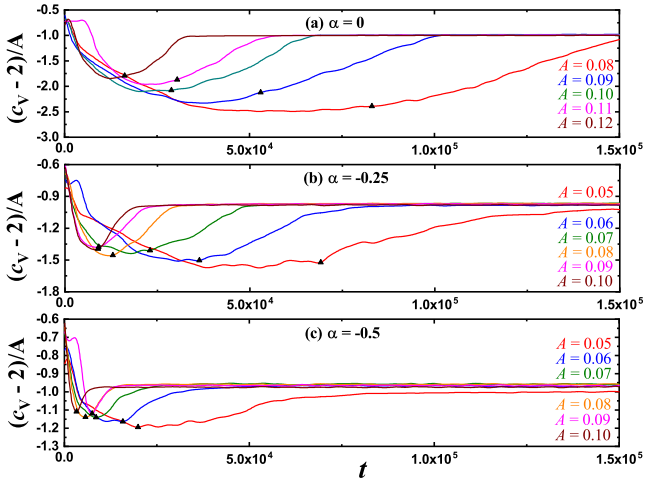

Figure 6: Specific heat normalized with respect to the zone-boundary mode amplitude A as the function of time for various values of A at three different values of the potential asymmetry parameter α. The black triangular markers indicate the corresponding values at maximal localization parameter L. It can be seen that specific heat is close to minimum when DBs are in the system and it increases as the system approaches thermal equilibrium.

B. Specific heat

The time-dependence of specific heat is plotted for the various mode amplitudes A in Fig. 6 for three different values of the potential asymmetry parameter α. We actually present the deviation of specific heat from its theoretical value of 2 for the linear system, normalized by A. The black triangular markers represent the values at which the localization parameter is maximal. From the comparison of Fig. 2 and Fig. 6, it can be seen that the specific heat is minimal when the the localization parameter is close to its maximum. During the transition to thermal equilibrium, the specific heat increases. From this, we conclude that the DBs resulting from the modulational instability of the zone-boundary mode reduce the specific heat of the chain. This can be explained quite simply as in our system with hard type anharmonicity, the DB frequency increases with its amplitude. Increase in the oscillation frequency results in an increase of particle velocities and thus, in their kinetic energies. Kinetic energy is in the denominator of Eq. (10) (which means there is an inverse proportionality between c_V and K) and hence its increase results in a decrease of c_V. Analogously, for the case of soft type anharmonicity, DB frequency decreases with its amplitude and the effect is just opposite, i.e., DBs increase the specific heat [77].

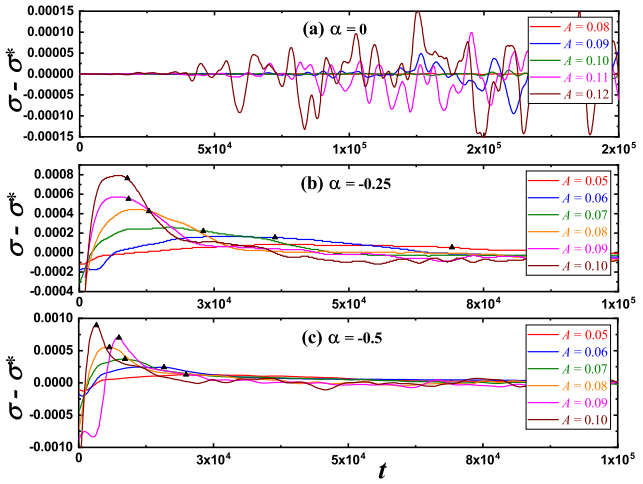

Figure 7: Stress as the function of time for various amplitudes of the initially excited zone-boundary mode at different values of the potential asymmetry parameter (α). The triangular markers indicate the corresponding values at maximal localization. The σ values have been normalized by subtracting the corresponding thermal equilibrium values $\sigma*$ to get the results in a comparable range.

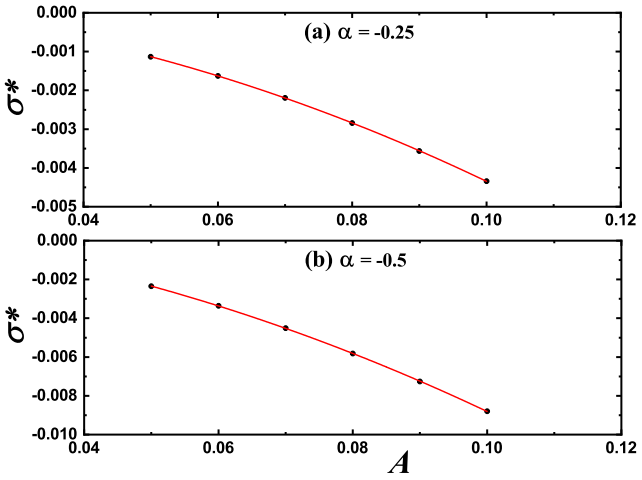

Figure 8: The Stress at thermal equilibrium as the function of Amplitude of the initially excited zone-boundary mode for different values of the potential asymmetry parameter (α).

C. Stress

The time-dependence of stress in the linear chain is plotted for the various mode amplitudes A in Fig. 7 for different values of the potential asymmetry parameter: (a) $\alpha = 0$, (b) $\alpha = -1/4$, and (c) $\alpha = -1/2$. We present here the deviation of stress σ from its value in thermal equilibrium, σ^*. For the symmetric potential ($\alpha = 0$) there is no thermal expansion and $\sigma^* = 0$. For negative values of α the dependence of σ^* on A is given in Fig. 8. In the limit of very small A, i.e., for the linear regime with small amplitude phonons, the stress is zero. For greater asymmetry, the absolute value of σ^* is larger for the same value of A [cf. (a) and (b)].

Coming back to Fig. 7, once again according to the position of the triangular markers or from the comparison of Fig. 2 and Fig. 7, it can be seen in (b) and (c) that the stress is maximal when the localization parameter is close to its maximum. During the transition to thermal equilibrium, the stress in the chain decreases.

Note that negative (compressive) stress appears in the system because its thermal expansion is suppressed by the use of periodic boundary conditions. In the chain with free ends, for negative α, thermal expansion at zero stress will be observed.

From this, we conclude that the DBs increase the stress in the FPU chain with periodic boundary conditions and in the case of free boundary conditions they will produce thermal expansion at zero stress.

D. Modulus of Elasticity

The time-dependence of the Young's modulus of elasticity E for the FPU chain is plotted for the various mode amplitudes A in Fig. 9 for (a) $\alpha = 0$, (b) $\alpha = -1/4$, and (c) $\alpha = -1/2$. Again, the difference between E and its value in thermal equilibrium, E^*, is given. The values of E^* for different amplitudes are plotted in Fig. 10 for (a) $\alpha = 0$, (b) $\alpha = -1/4$, and (c) $\alpha = -1/2$. From the comparison of Fig. 2 and Fig. 9, it can be seen that the modulus of elasticity is minimal when the localization parameter is maximal for $\alpha = 0$ and $\alpha = -0.25$. In the limit of very small A one has $E^* = 1$ and the compressive rigidity of the chain increases with increasing A almost equally for different values of α.

From Fig. 9, it can be seen that the effect of DBs on the Young's modulus is more pronounced for the symmetric potential ($\alpha = 0$). In this case, $E - E^*$ is minimal when DBs are in the system and it increases while the system approaches thermal equilibrium. From this, we conclude that the resulting DBs decrease the modulus of elasticity of the FPU chain with symmetric potential.

The effect of the Young's modulus reduction by DBs is much weaker for $\alpha = -1/4$ and this trend gets even reversed for $\alpha = -1/2$, i.e., in this case the modulus of elasticity is maximal when the localization parameter is maximal and decreases in thermal equilibrium. Thus, no definite conclusion can be made about the effect of DBs on the Young's modulus of the FPU chain with the asymmetric potential since it can be qualitatively different for different values of the asymmetry parameter.

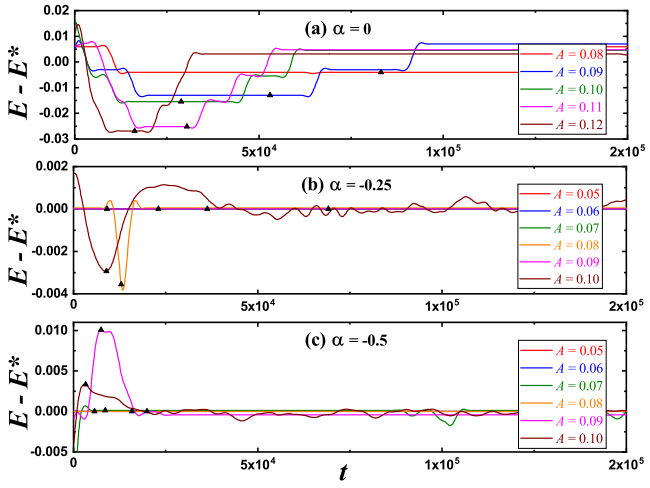

Figure 9: Modulus of elasticity as the function of time for various amplitudes of the initially excited zone-boundary mode at different values of the potential asymmetry parameter (α). The triangular markers indicate the corresponding values at maximal localization. The values of E have been normalized by subtracting the corresponding thermal equilibrium values E^* to get the results in a comparable range.

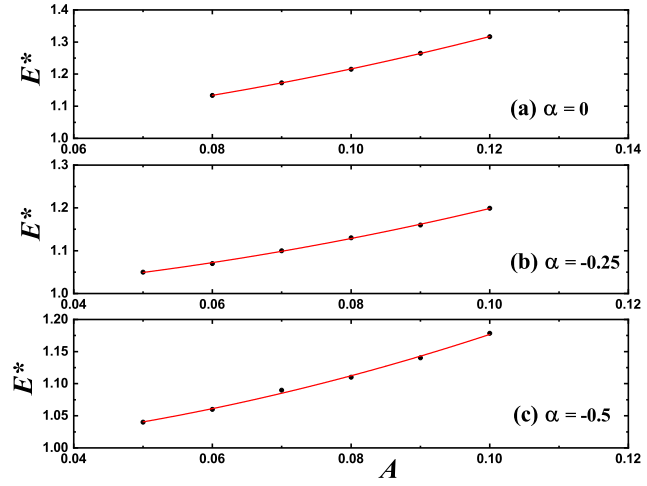

Figure 10: The Young's Modulus of elasticity at thermal equilibrium as the function of Amplitudes of the initially excited zone-boundary mode for different values of the potential asymmetry parameter (α).

IV. CONCLUSIONS

In the present study, the effect of DBs on different macroscopic properties of α-β-FPU chain was discussed. The properties such as specific heat, internal stress and Young's modulus were measured during the transition from modulationally unstable zone-boundary mode through the regime with high energy localization on DBs to thermal equilibrium.

It was found that for the chain with any set of parameters, specific heat is reduced by DBs. This is due to the hard type anharmonicity of the chain with DBs having greater vibrational frequencies for greater amplitudes. In the regime of energy localization by DBs, this leads to an increase in particles velocities and thus, their kinetic energies. Then, according to Eq. (10), an increase of kinetic energy in the DB regime results in the reduction of the specific heat. In the chains with soft type anharmonicity DB frequency drops with its amplitude and the effect is opposite, i.e., DBs increase the specific heat [77].

Internal stress in the chain with symmetric potential ($\alpha = 0$) does not appear since thermal expansion is observed only for asymmetric potentials. For negative α values considered in this study, negative (compressive) stress appears in the chain with periodic boundary conditions that suppress free thermal expansion. If free boundary conditions were used, thermal expansion of the chain at zero stress would be observed. The compressive stress is greater in the regime with DBs and thus, DBs increase thermal expansion of the FPU chain with negative α.

In the chain with symmetric potential, DBs reduce the Young's modulus, but with increasing asymmetry the effect gets weaker and for $\alpha = -1/2$ it becomes even reverse, i.e, an increase in modulus of elasticity is observed.

In future studies, it is planned to analyze the effect of DBs on macroscopic properties of two-dimensional nonlinear lattices supporting vibrational modes leading to modulational instability with formation of DBs.

Acknowledgments

The work of E.A.K. was supported by the Grant of the President of the Russian Federation for State support of young Russian scientists (No. MD-3639.2019.2). The work of V.A.G. was supported by the MEPhI Academic Excellence Project (Contract No. 02.a03.21.0005, 27.08.2013). S.V.D. acknowledges the support of the Russian Foundation for Basic Research, Grant No. 19-02-00971. The work was partly supported by the Tomsk State University competitiveness improvement programme and State assignment of IMCP RAS.

[1] A. S. Dolgov, Sov. Phys. Solid State **28**, 907 (1986).
[2] A. J. Sievers and S. Takeno, Intrinsic localized modes in anharmonic crystals, Phys. Rev. Lett. **61**, 970 (1988).
[3] J. B. Page, Asymptotic solutions for localized vibrational modes in strongly anharmonic periodic systems, Phys. Rev. B **41**, 7835 (1990).

[4] S. Flach and C. R. Willis, Discrete breathers, Phys. Rep. **295**, 181 (1998).

[5] S. Flach and A. V. Gorbach, Discrete breathers — Advances in theory and applications, Phys. Rep. **467**, 1 (2008).

[6] F. M. Russell, Y. Zolotaryuk, J. C. Eilbeck, and T. Dauxois, Moving breathers in a chain of magnetic pendulums, Phys. Rev. B **55**, 6304 (1997).

[7] J. Cuevas, L. Q. English, P. G. Kevrekidis, and M. Anderson, Discrete Breathers in a Forced-Damped Array of Coupled Pendula: Modeling, Computation, and Experiment, Phys. Rev. Lett. **102**, 224101 (2009).

[8] Y. Watanabe, T. Nishida, Y. Doi, and N. Sugimoto, Experimental demonstration of excitation and propagation of intrinsic localized modes in a mass-spring chain, Phys. Lett. A **382**, 1957 (2018).

[9] K. Vorotnikov, Y. Starosvetsky, G. Theocharis, and P. G. Kevrekidis, Wave propagation in a strongly nonlinear locally resonant granular crystal, Physica D **365**, 27 (2018).

[10] C. Chong, M. A. Porter, P. G. Kevrekidis, and C. Daraio, Nonlinear coherent structures in granular crystals, J. Phys.: Condens. Matter **29**, 413003 (2017).

[11] Y. Zhang, D. M. McFarland, and A. F. Vakakis, Propagating discrete breathers in forced one-dimensional granular networks: theory and experiment, Granular Matter **19**, 59 (2017).

[12] L. Liu, G. James, P. Kevrekidis, and A. Vainchtein, Breathers in a locally resonant granular chain with precompression, Physica D **331**, 27 (2016).

[13] L. Liu, G. James, P. Kevrekidis, and A. Vainchtein, Strongly nonlinear waves in locally resonant granular chains, Nonlinearity **29**, 3496 (2016).

[14] K. R. Jayaprakash, Y. Starosvetsky, A. F. Vakakis, M. Peeters, and G. Kerschen, Nonlinear normal modes and band zones in granular chains with no precompression, Nonlinear Dynam. **63**, 359 (2011).

[15] N. Boechler, G. Theocharis, S. Job, P. G. Kevrekidis, M. A. Porter, and C. Daraio, Discrete breathers in one-dimensional diatomic granular crystals, Phys. Rev. Lett. **104**, 244302 (2010).

[16] G. Theocharis, N. Boechler, P. G. Kevrekidis, S. Job, M. A. Porter, and C. Daraio, Intrinsic energy localization through discrete gap breathers in one-dimensional diatomic granular crystals, Phys. Rev. E **82**, 056604 (2010).

[17] M. Sato, B. E. Hubbard, and A. J. Sievers, Nonlinear energy localization and its manipulation in micromechanical oscillator arrays, Rev. Mod. Phys. **78**, 137 (2006).

[18] M. Sato, B. E. Hubbard, A. J. Sievers, B. Ilic, D. A. Czaplewski, and H. G. Craighead, Observation of locked intrinsic localized vibrational modes in a micromechanical oscillator array, Phys. Rev. Lett. **90**, 044102 (2003).

[19] M. Sato, B. E. Hubbard, A. J. Sievers, B. Ilic, and H. G. Craighead, Optical manipulation of intrinsic localized vibrational energy in cantilever arrays, Europhys. Lett. **66**, 318 (2004).

[20] R. Stearrett and L. Q. English, Experimental generation of intrinsic localized modes in a discrete electrical transmission line, J. Phys. D: Appl. Phys. **40**, 5394 (2007).

[21] A. Gomez-Rojas and P. Halevi, Discrete breathers in an electric lattice with an impurity: Birth, interaction, and death, Phys. Rev. E **97**, 022225 (2018).

[22] F. Palmero, L. Q. English, X.-L. Chen, W. Li, J. Cuevas-Maraver, and P. G. Kevrekidis, Experimental and numerical observation of dark and bright breathers in the band gap of a diatomic electrical lattice, Phys. Rev. E **99**, 032206 (2019).

[23] F. Lederer, G. I. Stegeman, D. N. Christodoulides, G. Assanto, M. Segev, and Y. Silberberg, Discrete solitons in optics, Phys. Rep. **463**, 1 (2008).

[24] P. Binder, D. Abraimov, A. V. Ustinov, S. Flach, and Y. Zolotaryuk, Observation of breathers in Josephson ladders, Phys. Rev. Lett. **84**, 745 (2000).

[25] E. Trias, J. J. Mazo, and T. P. Orlando, Discrete breathers in nonlinear lattices: experimental detection in a Josephson array, Phys. Rev. Lett. **84**, 741 (2000).

[26] S. V. Dmitriev, E. A. Korznikova, J. A. Baimova, and M. G. Velarde, Discrete breathers in crystals, Phys. Usp. **59**, 446 (2016).

[27] B. Mihaila *et al.*, Pinning frequencies of the collective modes in α-uranium, Phys. Rev. Lett. **96**, 076401 (2006).

[28] M.E. Manley *et al.*, Formation of a new dynamical mode in α-uranium observed by inelastic X-ray and neutron scattering, Phys. Rev. Lett. **96**, 125501 (2006).

[29] M. E. Manley *et al.*, Intrinsically localized vibrations and the mechanical properties of α-uranium, J. Alloys Compd. **444**, 129 (2007).

[30] T. Markovich, E. Polturak, J. Bossy, and E. Farhi, Observation of a new excitation in bcc ^{4}He by inelastic neutron scattering, Phys. Rev. Lett. **88**, 195301 (2002).

[31] M. E. Manley *et al.*, Intrinsic localized modes observed in the high-temperature vibrational spectrum of NaI, Phys. Rev. B **79**, 134304 (2009).

[32] M. E. Manley, D. L. Abernathy, N. I. Agladze, and A. J. Sievers, Symmetry-breaking dynamical pattern and localization observed in the equilibrium vibrational spectrum of NaI, Sci. Rep. **1**, 4 (2011).

[33] W. Liang, G. M. Vanacore, and A. H. Zewail, Observing (non)linear lattice dynamics in graphite by ultrafast Kikuchi diffraction, Proc. Natl. Acad. Sci. USA **111**, 5491 (2014).

[34] M. E. Manley *et al.*, Intrinsic anharmonic localization in thermoelectric PbSe, Nature Commun. **10**, 1928 (2019).

[35] A. J. Sievers, M. Sato, J. B. Page, and T. Rössler, Thermally populated intrinsic localized modes in pure alkali halide crystals, Phys. Rev. B **88**, 104305 (2013).

[36] G. M. Chechin, S. V. Dmitriev, I. P. Lobzenko, and D. S. Ryabov, Properties of discrete breathers in graphane from *ab initio* simulations, Phys. Rev. B **90**, 045432 (2014).

[37] I. P. Lobzenko, G. M. Chechin, G. S. Bezuglova, Yu. A. Baimova, E. A. Korznikova, and S. V. Dmitriev, Ab initio simulation of gap discrete breathers in strained graphene, Phys. Solid State **58**, 633 (2016).

[38] S. A. Kiselev and A. J. Sievers, Generation of intrinsic vibrational gap modes in three-dimensional ionic crystals, Phys. Rev. B **55**, 5755 (1997).

[39] L. Z. Khadeeva and S. V. Dmitriev, Discrete breathers in crystals with NaCl structure, Phys. Rev. B **81**, 214306 (2010).

[40] A. Riviere, S. Lepri, D. Colognesi, and F. Piazza, Wavelet imaging of transient energy localization in nonlinear systems at thermal equilibrium: The case study of NaI crystals at high temperature, Phys. Rev. B **99**, 024307 (2019).

[41] A. A. Kistanov, R. T. Murzaev, S. V. Dmitriev, V. I. Dubinko, and V. V. Khizhnyakov, Moving discrete breathers in a monoatomic two-dimensional crystal, JETP Lett. **99**, 353 (2014).

[42] E. A. Korznikova, S. Yu. Fomin, E. G. Soboleva, and S. V. Dmitriev, Highly symmetric discrete breather in a two-dimensional Morse crystal, JETP Lett. **103**, 277 (2016).

[43] N. K. Voulgarakis, G. Hadjisavvas, P. C. Kelires, and G. P. Tsironis, Computational investigation of intrinsic localization in crystalline Si, Phys. Rev. B **69**, 113201 (2004).

[44] R. T. Murzaev, D. V. Bachurin, E. A. Korznikova, and S. V. Dmitriev, Localized vibrational modes in diamond, Phys. Lett. A **381**, 1003 (2017).

[45] M. Haas, V. Hizhnyakov, A. Shelkan, M. Klopov, and A. J. Sievers, Prediction of high-frequency intrinsic localized modes in Ni and Nb, Phys. Rev. B **84**, 144303 (2011).

[46] O. V. Bachurina, Linear discrete breather in fcc metals, Comp. Mater. Sci. **160**, 217 (2019).

[47] O. V. Bachurina, Plane and plane-radial discrete breathers in fcc metals, Model. Simul. Mater. Sci. Eng. **27**, 055001 (2019).

[48] R. T. Murzaev, A. A. Kistanov, V. I. Dubinko, D. A. Terentyev, and S. V. Dmitriev, Moving discrete breathers in bcc metals V, Fe and W, Comp. Mater. Sci. **98**, 88 (2015).

[49] D. A. Terentyev, A. V. Dubinko, V. I. Dubinko, S. V. Dmitriev, E. E. Zhurkin, and M. V. Sorokin, Interaction of discrete breathers with primary lattice defects in bcc Fe, Model. Simul. Mater. Sc. **23**, 085007 (2015).

[50] R. T. Murzaev, R. I. Babicheva, K. Zhou, E. A. Korznikova, S. Y. Fomin, V. I. Dubinko, and S. V. Dmitriev, Discrete breathers in alpha-uranium, Eur. Phys. J. B **89**, 168 (2016).

[51] O. V. Bachurina, R. T. Murzaev, A. S. Semenov, E. A. Korznikova, and S. V. Dmitriev, Properties of moving discrete breathers in beryllium, Phys. Solid State **60**, 989 (2018).

[52] N. N. Medvedev, M. D. Starostenkov, and M. E. Manley, Energy localization on the *Al* sublattice of Pt_3Al with $L1_2$ order, J. Appl. Phys. **114**, 213506 (2013).

[53] M. D. Starostenkov, A. I. Potekaev, S. V. Dmitriev, P. V. Zakharov, A. M. Eremin, and V. V. Kulagina, Dynamics of discrete breathers in a Pt_3Al crystal, Russ. Phys. J. **58**, 1353 (2016).

[54] V. Dubinko, D. Laptev, D. Terentyev, S. V. Dmitriev, and K. Irwin, Assessment of discrete breathers in the metallic hydrides, Comp. Mater. Sci. **158**, 389 (2019).

[55] P. V. Zakharov, E. A. Korznikova, S. V. Dmitriev, E. G. Ekomasov, and K. Zhou, Surface discrete breathers in Pt_3Al intermetallic alloy, Surf. Sci. **679**, 1 (2019).

[56] J. A. Baimova, E. A. Korznikova, I. P. Lobzenko, and S. V. Dmitriev, Discrete breathers in carbon and hydrocarbon nanostructures, Rev. Adv. Mater. Sci. **42**, 68 (2015).

[57] E. A. Korznikova, J. A. Baimova, and S. V. Dmitriev, Effect of strain on gap discrete breathers at the edge of armchair graphene nanoribbons, Europhys. Lett. **102**, 60004 (2013).

[58] B. Liu, J. A. Baimova, S. V. Dmitriev, X. Wang, H. Zhu, and K. Zhou, Discrete breathers in hydrogenated graphene, J. Phys. D: Appl. Phys. **46**, 305302 (2013).

[59] J. A. Baimova, S. V. Dmitriev, and K. Zhou, Discrete breather clusters in strained graphene, Europhys. Lett. **100**, 36005 (2012).

[60] E. A. Korznikova, A. V. Savin, Yu. A. Baimova, S. V. Dmitriev, and R. R. Mulyukov, Discrete breather on the edge of the graphene sheet with the armchair orientation, JETP Lett. **96**, 222 (2012).

[61] A. V. Savin and Yu. S. Kivshar, Nonlinear breatherlike localized modes in C_{60} nanocrystals, Phys. Rev. B **85**, 125427 (2012).

[62] T. Shimada, D. Shirasaki, and T. Kitamura, Stone-Wales transformations triggered by intrinsic localized modes in carbon nanotubes, Phys. Rev. B **81**, 035401 (2010).

[63] Y. Yamayose, Y. Kinoshita, Y. Doi, A. Nakatani, and T. Kitamura, Excitation of intrinsic localized modes in a graphene sheet, Europhys. Lett. **80**, 40008 (2007).

[64] Y. Kinoshita, Y. Yamayose, Y. Doi, A. Nakatani, and T. Kitamura, Selective excitations of intrinsic localized modes of atomic scales in carbon nanotubes, Phys. Rev. B **77**, 024307 (2008).

[65] Y. Doi and A. Nakatani, Numerical study on unstable perturbation of intrinsic localized modes in graphene, J. Solid Mech. Mater. Eng. **6**, 71 (2012).

[66] L. Z. Khadeeva, S. V. Dmitriev, and Yu. S. Kivshar, Discrete breathers in deformed graphene, JETP Lett. **94**, 539 (2011).

[67] I. Evazzade, I. P. Lobzenko, E. A. Korznikova, I. A. Ovid'Ko, M. R. Roknabadi, and S. V. Dmitriev, Energy transfer in strained graphene assisted by discrete breathers excited by external ac driving, Phys. Rev. B **95**, 035423 (2017).

[68] E. Barani, I. P. Lobzenko, E. A. Korznikova, E. G. Soboleva, S. V. Dmitriev, K. Zhou, and A. M. Marjaneh, Transverse discrete breathers in unstrained graphene Eur. Phys. J. B, **90**, 38 (2017).

[69] E. Barani, E. A. Korznikova, A. P. Chetverikov, K. Zhou, and S. V. Dmitriev, Gap discrete breathers in strained boron nitride, Phys. Lett. A **381**, 3553 (2017).

[70] B. Juanico, Y.-H. Sanejouand, F. Piazza, and P. De Los Rios, Discrete Breathers in Nonlinear Network Models of Proteins, Phys. Rev. Lett. **99**, 238104 (2007).

[71] F. Piazza and Y.-H. Sanejouand, Discrete breathers in protein structures, Phys. Biol. **5**, 026001 (2008).

[72] M. Peyrard, S. Cuesta-López, and G. James, Nonlinear analysis of the dynamics of DNA breathing, J. Biol. Phys. **35**, 73 (2009).

[73] A. P. Chetverikov, K. S. Sergeev, and V. D. Lakhno, Trapping and transport of charges in DNA by mobile discrete breathers, Math. Biol. Bioinf. **13**, t59 (2018).

[74] M. E. Manley, Impact of intrinsic localized modes of atomic motion on materials properties, Acta Mater. **58**, 2926 (2010).

[75] Y. Ming, D.-B. Ling, H.-M. Li, and Z.-J. Ding, Energy thresholds of discrete breathers in thermal equilibrium and relaxation processes, Chaos **27**, 063106 (2017).

[76] D. Xiong, D. Saadatmand, and S. V. Dmitriev, Crossover from ballistic to normal heat transport in the ϕ^4 lattice: If nonconservation of momentum is the reason, what is the mechanism?, Phys. Rev. E **96**, 042109 (2017).

[77] M. Singh, A. Y. Morkina, E. A. Korznikova, V. I. Dubinko, D. A. Terentiev, D. Xiong, O. B. Naimark, V. A. Gani, S. V. Dmitriev, Effect of discrete breathers on the specific heat of a nonlinear chain, arXiv:1907.03280 [nlin.PS] (2019).

[78] V. M. Burlakov and S. Kiselev, Molecular-dynamics simulation of the decay kinetics of uniform excitation of an anharmonic 1D chain, Sov. Phys. JETP **72**, 854 (1991).
[79] V. V. Mirnov, A. J. Lichtenberg, and H. Guclu, Chaotic breather formation, coalescence, and evolution to energy equipartition in an oscillatory chain, Physica D **157**, 251 (2001).
[80] K. Ullmann, A. J. Lichtenberg, and G. Corso, Energy equipartition starting from high-frequency modes in the Fermi–Pasta–Ulam β oscillator chain, Phys. Rev. E **61**, 2471 (2000).
[81] Yu. A. Kosevich and S. Lepri, Modulational instability and energy localization in anharmonic lattices at finite energy density, Phys. Rev. B **61**, 299 (2000).
[82] T. Cretegny, T. Dauxois, S. Ruffo, and A. Torcini, Localization and equipartition of energy in the β-FPU chain: Chaotic breathers, Physica D **121**, 109 (1998).
[83] K. Ikeda, Y. Doi, B. F. Feng, and T. Kawahara, Chaotic breathers of two types in a two-dimensional Morse lattice with an on-site harmonic potential, Physica D **225**, 184 (2007).
[84] L. Kavitha, A. Mohamadou, E. Parasuraman, D. Gopi, N. Akila, and A. Prabhu, Modulational instability and nano-scale energy localization in ferromagnetic spin chain with higher order dispersive interactions, J. Magn. Magn. Mat. **404**, 91 (2016).
[85] L. Kavitha, E. Parasuraman, D. Gopi, A. Prabhu, and R. A. Vicencio, Nonlinear nano-scale localized breather modes in a discrete weak ferromagnetic spin lattice, J. Magn. Magn. Mat. **401**, 394 (2016).
[86] B. Tang and K. Deng, Discrete breathers and modulational instability in a discrete ϕ^4 nonlinear lattice with next-nearest-neighbor couplings, Nonlinear Dyn. **88**, 2417 (2017).
[87] E. A. Korznikova, D. V. Bachurin, S. Yu. Fomin, A. P. Chetverikov, and S. V. Dmitriev, Instability of vibrational modes in hexagonal lattice, Eur. Phys. J. B **90**, 23 (2017).
[88] S. Flach, A. Gorbach, Discrete breathers in Fermi-Pasta-Ulam lattices, Chaos **15**, 015112 (2005).
[89] D. Saadatmand, D. Xiong, V. A. Kuzkin, A. M. Krivtsov, A. V. Savin, and S. V. Dmitriev, Discrete breathers assist energy transfer to ac-driven nonlinear chains, Phys. Rev. E **97**, 022217 (2018).